Supplementary Information

TNF Antagonist Sensitizes Synovial Fibroblasts to Ferroptotic Cell Death in Collagen-induced Arthritis Mouse Models

First Authors: Jiao Wu, Zhuan Feng, Liang Chen, Yong Li
Corresponding Authors: Jiao Wu, Xuejun Jiang, Zhi-Nan Chen & Ping Zhu

Supplementary Figures 1-12

Supplementary Tables 1-7

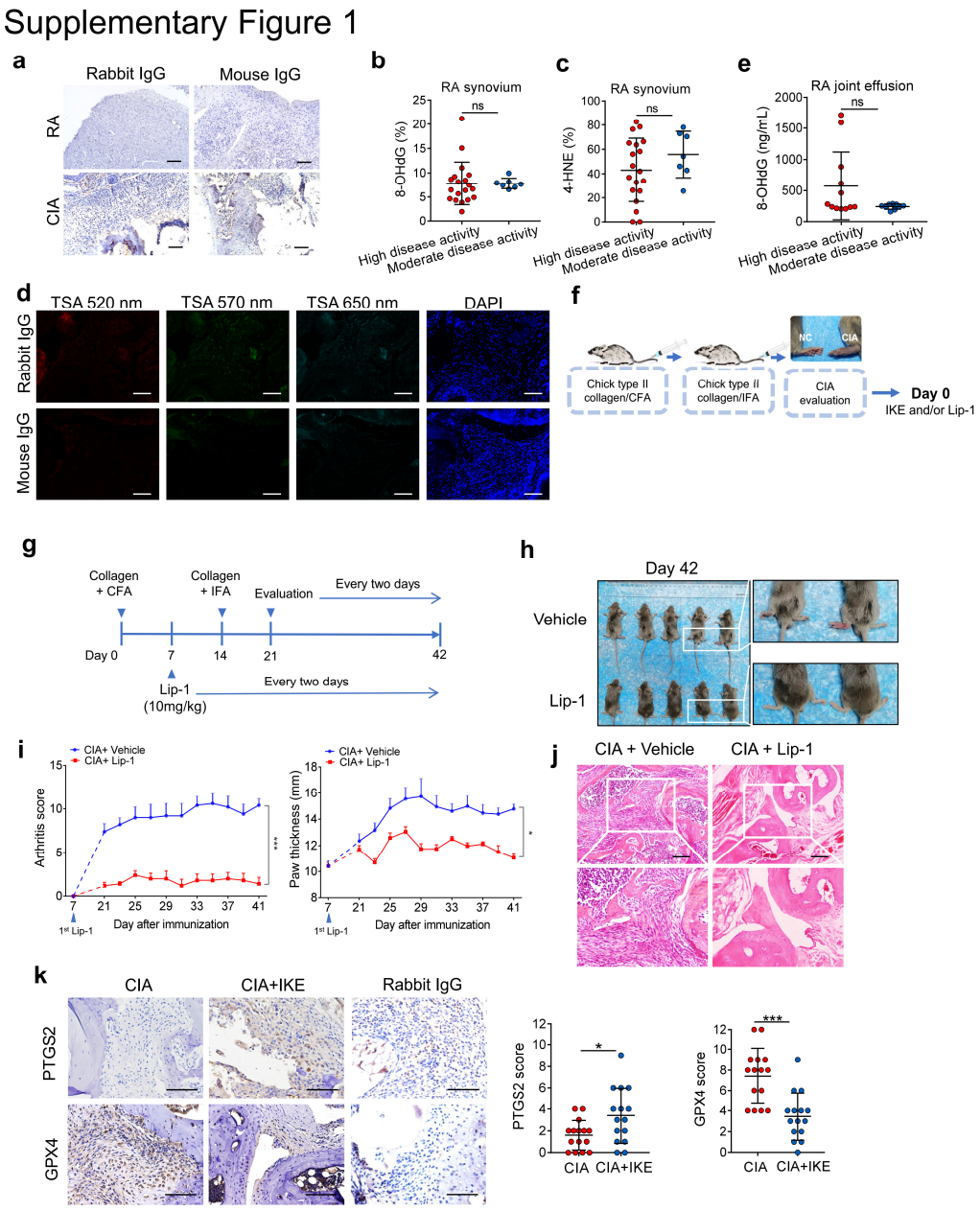

Supplementary Fig. 1. IKE induces ferroptosis in fibroblast populations from the synovium of RA patients. a Immunohistochemistry on formalin-fixed paraffin embedded human RA synovium or mouse CIA joints using 10 μg/mL of rabbit IgG1 isotype control or mouse IgG1 isotype control followed by an anti-mouse/rabbit avidin-biotin HRP detection system. Nuclei are counterstained with hematoxylin. Scale bars, 100 μm. The isotype control was repeated independently along with the staining of different molecules with similar results. **b** Quantitative comparison of 8-OHdG staining in the synovium of RA patients with different disease activities. High disease activity, n = 19 RA patients; moderate disease activity, n = 7 RA patients. ns, P = 0.9846; two-tailed t test. **c** Quantitative comparison of 4-HNE staining in the synovium of RA patients with different disease activities. High disease activity, n = 19 RA patients; moderate disease activity, n = 7 RA patients. ns, P = 0.2505; two-tailed t test. **d** Fluorescent multiplex IHC staining of mouse CIA joints using 10 μg/mL of rabbit IgG1 isotype control or mouse IgG1

isotype control followed by TSA detection kit. Scale bars, 200 μm. The isotype control was repeated independently along with the staining of different molecules with similar results. **e** 8-OHdG concentration in the joint fluid of RA patients with different disease activities. High disease activity, n = 12 RA patients; moderate disease activity, n = 8 RA patients. ns, $P = 0.0853$; two-tailed t test. **f** Establishment of a CIA mouse model and administration of IKE and/or Lip-1 treatment. **g** Establishment of a CIA mouse model and administration of Lip-1 treatment started before the shown up of significant phenotype of arthritis. **h** Representative images of the paws from mice with or without administration of Lip-1 42 days after immunization with type II collagen. **i** Joint inflammation measured by arthritis score (left) and paw thickness (right) in CIA model mice that were intraperitoneally injected with Lip-1 every two days for 5 weeks. $^{***}P = 0.0008$, $^{*}P = 0.0111$; two-way repeated measure ANOVA. n = 5 mice for each group. **j** H&E staining images of representative joints in CIA model mice with or without administration of Lip-1. Scale bars, 100 μm. Similar results were observed from 15 joints tested for each group. **k** Immunohistochemical staining and scoring of PTGS2 and GPX4 in the joints of CIA model mice. n = 15 joints for each group. $^{*}P = 0.0228$, $^{***}P = 0.0002$; two-tailed t test. Scale bars, 100 μm. Data in **i** are presented as mean ± SEM. Other data are presented as mean ± SD. Source data are provided as a Source Data file.

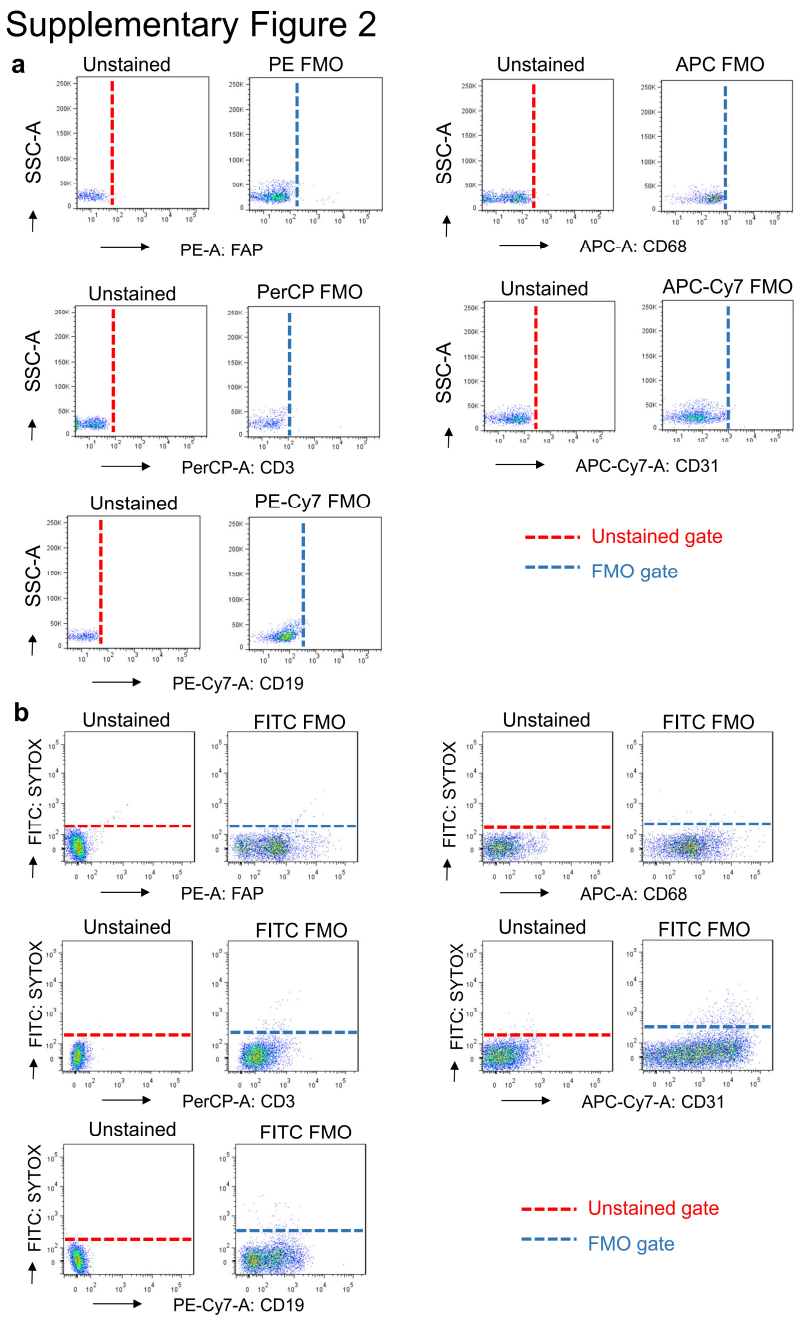

Supplementary Fig. 2. FMO controls used in Fig. 2c. a FMO for PE-FAPα, APC-CD68, PerCP-CD3, APC-Cy7-CD31 and PE-Cy7-CD19. **b** FMO for SYTOX Green.

Supplementary Figure 3

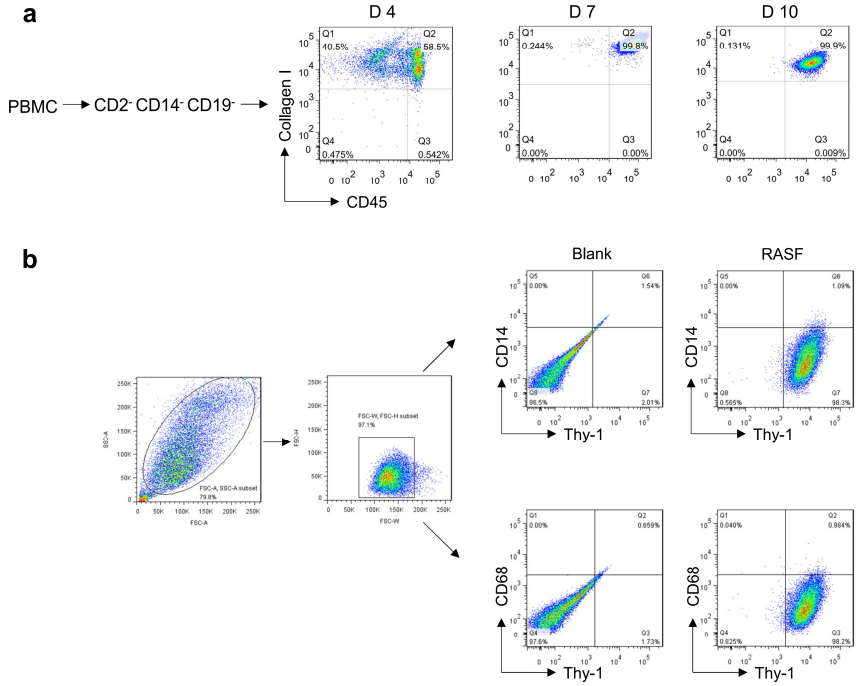

Supplementary Fig. 3. Isolation and identification of circulating fibroblasts and synovial fibroblasts. a CD2-CD14-CD19- cells from PBMCs of RA patients were cultured for the indicated times, and the percentages of CD45+ Collagen 1+ cells were analyzed by flow cytometry. **b** Flow cytometric analysis of digested synovial cells cultured from RA patients, and fibroblasts were identified as the CD14- CD68- Thy1+ population by flow cytometry.

Supplementary Figure 4

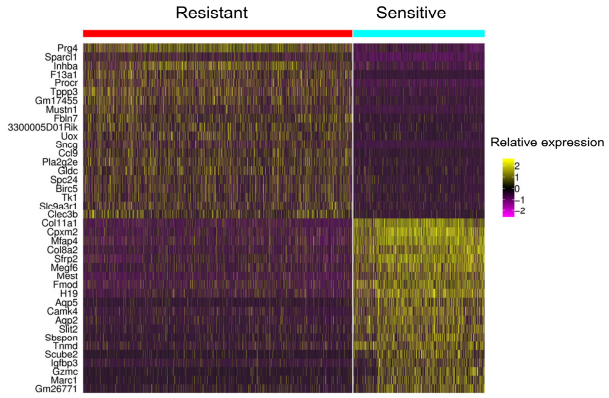

Supplementary Fig. 4. Differential gene expression of ferroptosis-sensitive and ferroptosis-resistant fibroblast subsets. The heat map shows the expression of the top 20 genes (by *P* value) discovered that were considered significant and conserved marker genes for each subset.

Supplementary Figure 5

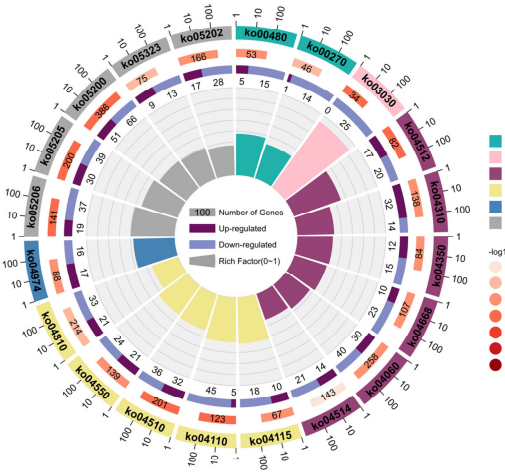

ID	Description
ko00480	Glutathione metabolism
ko00270	Cysteine and methionine metabolism
ko03030	DNA replication
ko04668	TNF signaling pathway
ko04512	ECM-receptor interaction
ko04310	Wnt signaling pathway
ko04350	TGF-beta signaling pathway
ko04060	Cytokine-cytokine receptor interaction
ko04060	Cell adhesion molecules (CAMs)
ko04115	p53 signaling pathway
ko04110	Cell cycle
ko04510	Focal adhesion
ko04550	Signaling pathways regulating pluripotency of stem cells
ko04810	Regulation of actin cytoskeleton
ko04974	Protein digestion and absorption
ko05206	MicroRNAs in cancer
ko05205	Proteoglycans in cancer
ko05200	Pathways in cancer
ko05323	Rheumatoid arthritis
ko05202	Transcriptional misregulation in cancers

Supplementary Fig. 5. KEGG (Kyoto Encyclopedia of Genes and Genomes) enrichment analysis of differentially expressed genes in ferroptosis-sensitive and ferroptosis-resistant fibroblast subsets. The first lap indicates the KEGG pathway; the second lap indicates the number of genes in the genome background and -log10 Q values for enrichment of the differentially expressed genes for the KEGG pathway; the third lap indicates the ratio of the upregulated genes (purple) and downregulated genes (blue); and the fourth lap indicates the rich factor of each pathway.

Supplementary Figure 6

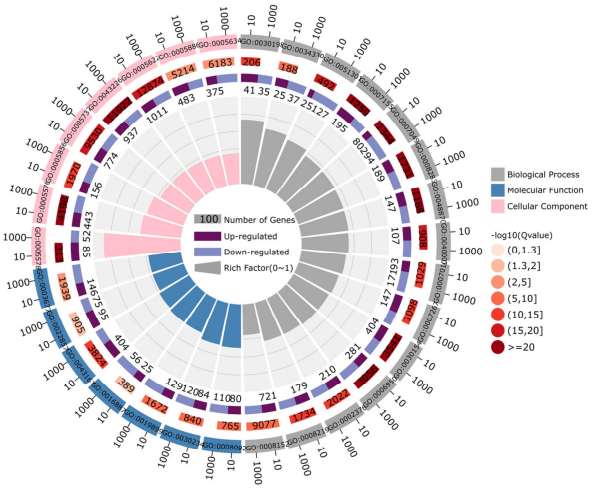

ID	Description
GO:0008219	cell death
GO:0006950	response to stress
GO:0008283	cell proliferation
GO:0051301	cell division
GO:0040007	growth
GO:0007049	cell cycle
GO:0007155	cell adhesion
GO:0048870	cell motility
GO:0030198	extracellular matrix organization
GO:0034330	cell junction organization
GO:0007010	cytoskeleton organization
GO:0007267	cell-cell signaling
GO:0008152	metabolic process
GO:0002376	immune system process
GO:0030154	cell differentiation
GO:0043167	ion binding
GO:0008092	cytoskeletal protein binding
GO:0030234	enzyme regulator activity
GO:0019899	enzyme binding
GO:0003677	DNA binding
GO:0016887	ATPase activity
GO:0022857	transmembrane transporter activity
GO:0005576	extracellular region
GO:0005578	proteinaceous extracellular matrix
GO:0043226	organelle
GO:0005622	intracellular
GO:0005737	cytoplasm
GO:0005856	cytoskeleton
GO:0005634	nucleus
GO:0005886	plasma membrane

Supplementary Fig. 6. GO (Gene Ontology) enrichment analysis of differentially expressed genes in ferroptosis-sensitive and ferroptosis-resistant fibroblast subsets.

Supplementary Figure 7

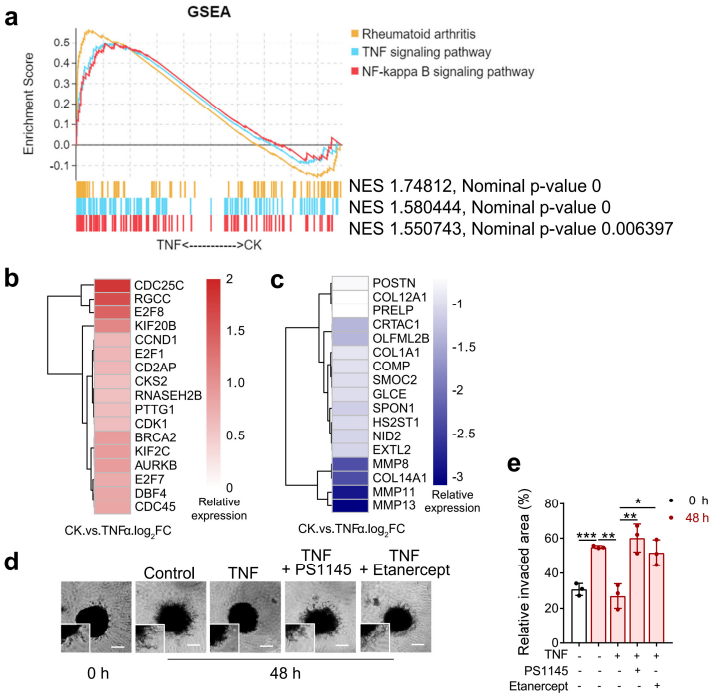

Supplementary Fig. 7. Long-term exposure of fibroblasts to TNF increases the proliferation potential and decreases the genes related to extracellular matrix in fibroblasts. a-c Fibroblasts were stimulated with TNF (20 ng/ml) for 96 h, and RNA sequencing was performed. **a** Enrichment plots of GO_Rheumatoid, TNF signaling pathway and NF-κB signaling pathway gene sets among TNF-stimulated fibroblasts compared to control fibroblasts as identified by GSEA. The p-value is calculated through permutation tests. **b** Genes enriched in the GO_Cell division gene set (left) and KEGG_DNA replication gene set among the ferroptosis-resistant subset were cross-referenced against genes that showed increased expression after TNF treatment of fibroblasts from individuals with RA, and the expression of selected mRNA transcripts is shown. **c** Genes enriched in the GO_Proteinaceous extracellular matrix gene set (left) and KEGG_Glycosaminoglycan biosynthesis gene set among the ferroptosis-sensitive subset were cross-referenced against genes that were decreased after treatment of RA fibroblasts with TNF, and the expression of selected mRNA transcripts is shown. **d** Representative images of fibroblast spheroids grown in Matrigel and treated with TNF, PS1145 and etanercept for the indicated times. Scale bars, 100 μm. **e** The protrusion area extruded from the main body of the spheroid was monitored. n = 3 biologically independent samples per condition. ***P = 0.0003; **P = 0.0023, 0.0058 (left to right); *P = 0.0135; two-tailed t-test. All data are presented as mean ± SD. Source data are provided as a Source Data file.

Supplementary Figure 8

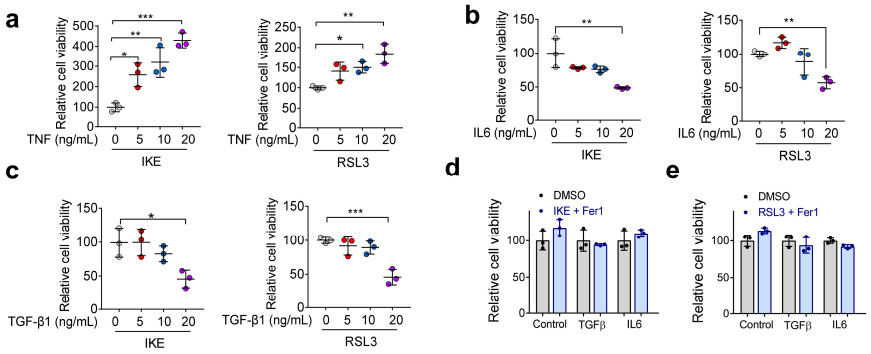

Supplementary Fig. 8. TNF protects fibroblasts against ferroptosis, while IL-6 and TGF-β sensitize fibroblasts to ferroptosis. a-c Relative viability of fibroblasts from individuals with RA that are primed with different concentrations of TNF (**a**), IL-6 (**b**) and TGF-β (**c**), followed by treatment with IKE (1 μM, 28 h) or RSL3 (0.125 μM, 14 h). n = 3 biologically independent samples per condition. **a** Left, * $P = 0.0231$, ** $P = 0.0035$, *** $P = 0.0002$. Right, * $P = 0.0384$, ** $P = 0.0020$; one-way ANOVA followed by multiple comparisons. **b** Left, ** $P = 0.0022$. Right, ** $P = 0.0097$; one-way ANOVA followed by multiple comparisons. **c** Left, * $P = 0.0205$. Right, *** $P = 0.0009$; one-way ANOVA followed by multiple comparisons. **d-e** Relative viability of fibroblasts primed with TGF-β or IL-6, followed by treatment with IKE (**d**) or RSL3 (**e**) in the presence of Fer1. n = 3 biologically independent samples per condition. All data are presented as mean ± SD. Source data are provided as a Source Data file.

Supplementary Figure 9

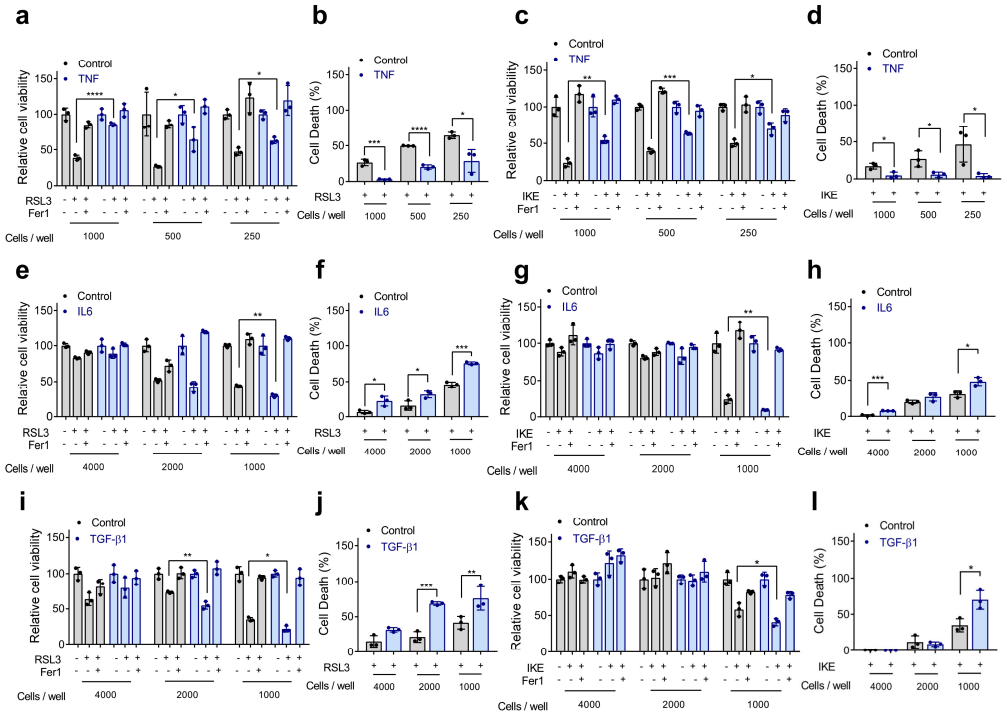

Supplementary Fig. 9. TNF reduces ferroptosis susceptibility in a cell density-independent manner. a-d Fibroblasts from individuals with RA were seeded at the indicated density in 96-well plates and primed with TNF. Relative viability was measured after RSL3 treatment for 12 h (**a**) or IKE treatment for 26 h (**c**), and cell death was measured after RSL3 treatment for 10 h (**b**) or IKE treatment for 24 h (**d**). Cells were stained with hoechst 33342 (0.1 μg/mL) to monitor total cell number, and with SYTOX green (5 nM) to monitor cell death. **a** ****$P < 0.0001$, *$P = 0.0194$, 0.0171 (left to right); two-tailed t-test. **b** *** $P = 0.0009$, ****$P < 0.0001$, *$P = 0.0198$; two-tailed t-test. **c** ** $P = 0.0018$, ***$P = 0.0002$, *$P = 0.0280$; two-tailed t-test. **d** *$P = 0.0215$, 0.0325, 0.0382 (left to right); two-tailed t-test. **e-h** Fibroblasts from individuals with RA and set at the indicated density were primed with IL-6 and then treated with RSL3 or IKE, and relative cell viability and cell death were measured as described above. **e** **$P = 0.0010$; two-tailed t-test. **f** *$P = 0.0217$, 0.0277 (left to right), *** $P = 0.0002$; two-tailed t-test. **g** ** $P = 0.0012$; two-tailed t-test. **h** ***$P = 0.0003$, *$P = 0.0115$; two-tailed t-test. **i-l** Fibroblasts from individuals with RA and set at the indicated density were primed with TGF-β and then treated with RSL3 or IKE, and relative cell viability and cell death were measured as described above. **i** **$P = 0.0045$, *$P = 0.0107$; two-tailed t-test. **j** ***$P = 0.0005$, ** $P = 0.0021$; two-tailed t-test. **k** * $P = 0.0465$; two-tailed t-test. **l** *$P = 0.0182$; two-tailed t-test. n = 3 biologically independent samples per condition. All data are presented as mean ± SD. Source data are provided as a Source Data file.

Supplementary Figure 10

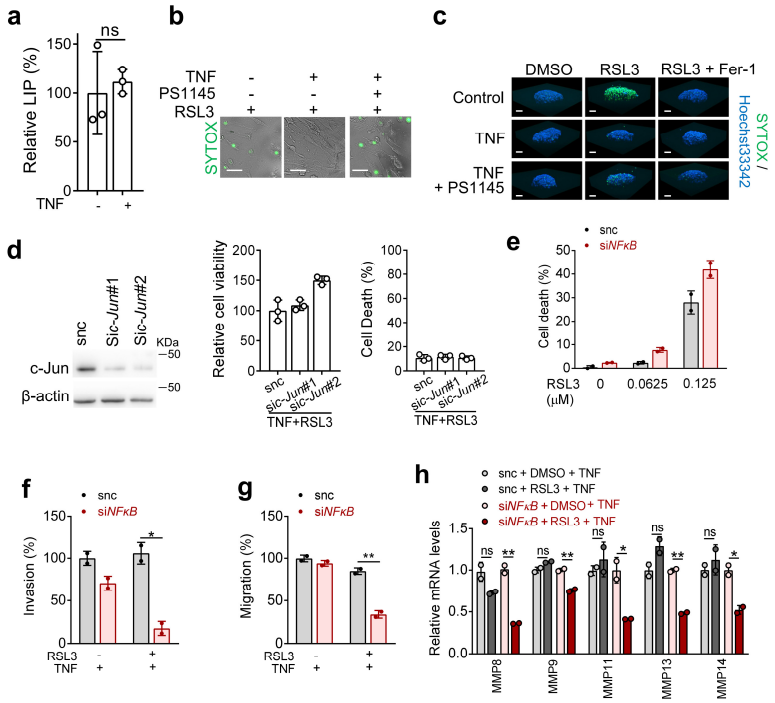

Supplementary Fig. 10. Sublethal doses of ferroptosis-inducers modulates the aggressive behaviors of RA fibroblasts. a Cellular labile iron pool (LIP) level in fibroblasts treated with TNF. n = 3 biologically independent samples per condition. ns, P = 0.6721; two-tailed t test. **b** Microscopy showing cell death. Scale bars, 20 μm. Similar results were observed from 3 times independent experiments. **c** Three-dimensional spheroids formed by fibroblasts were treated as indicated. Dead cells were stained with SYTOX green, while all nuclei were stained with Hoechst 33342 (blue). Scale bars, 100 μm. **d** Left, western blotting analysis of c-Jun expression in fibroblasts transfected with scramble siRNA or either of two independent siRNAs targeting c-Jun, which is a component of AP-1 (si*c-Jun*#1, si*c-Jun*#2). Right, relative viability and cell death of fibroblasts transfected with scramble siRNA or siRNA targeting c-Jun and treated with TNF followed by RSL3. n = 3 biologically independent samples per condition. **e** Cell death of fibroblasts transfected with scramble siRNA or siRNA targeting NF-κB p65, and then treated with indicated concentrations of RSL3. n = 2 biologically independent samples per condition. **f-g** Invasive (**f**) and migrative (**g**) potentials of RA fibroblasts transfected with scramble siRNA or siRNA targeting NF-κB p65, and then treated with TNF followed by RSL3 (0.0625 μM), measured by the transwell assay. n = 2 biologically independent samples per condition. *P = 0.0147, **P = 0.0065; two-tailed t test. **h** The mRNA levels of MMP8, -9, -11, -13 and -14 in NF-κB p65 knockdown fibroblasts with TNF and RSL3 treatment. n = 2 biologically independent samples per condition. ns, P = 0.0911, 0.0644, 0.4768, 0.1108, 0.4827 (left to right); *P = 0.0324, 0.0195 (left to right); **P = 0.0049, 0.0072, 0.0015 (left to right); two-tailed t test. All data are presented as mean ± SD. Source data are provided as a Source Data file.

Supplementary Figure 11

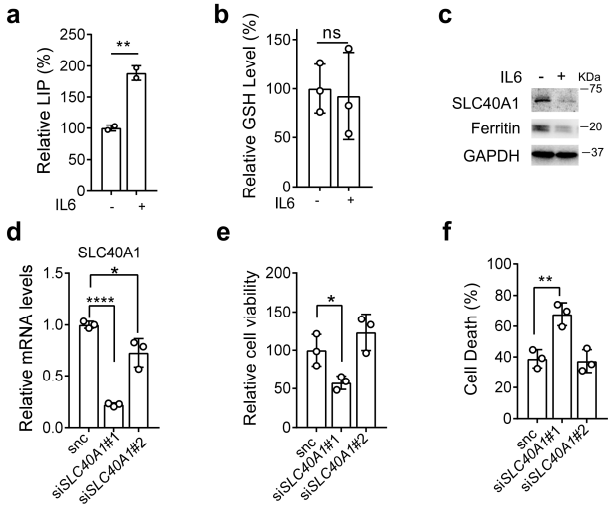

Supplementary Fig. 11. IL-6 sensitized fibroblasts to ferroptosis. a The LIP level in fibroblasts treated with IL-6. n = 2 biologically independent samples per condition. ***P* = 0.0098; two-tailed t test. **b** Intracellular GSH in fibroblasts treated with IL-6 for 72 h. n = 3 biologically independent samples per condition. ns, *P* = 0.8078; two-tailed t test. **c** Western blotting analysis of SLC40A1 and Ferritin expression in fibroblasts stimulated with IL-6 for 72 h. **d** Relative mRNA levels of SLC40A1 in fibroblasts transfected with scramble siRNA or either of two independent siRNAs targeting SLC40A1 (siSLC40A1#1, siSLC40A1#2). n = 3 biologically independent samples per condition. **P* = 0.0162, *****P* < 0.0001; one-way ANOVA followed by multiple comparisons. **e-f** Relative viability (**e**) and cell death (**f**) of fibroblasts transfected with scramble siRNA or siRNA targeting SLC40A1and treated with IL-6 followed by RSL3. n = 3 biologically independent samples per condition. **P* = 0.0312, ***P* = 0.0063; two-tailed t test. All data are presented as mean ± SD. Source data are provided as a Source Data file.

Supplementary Figure 12

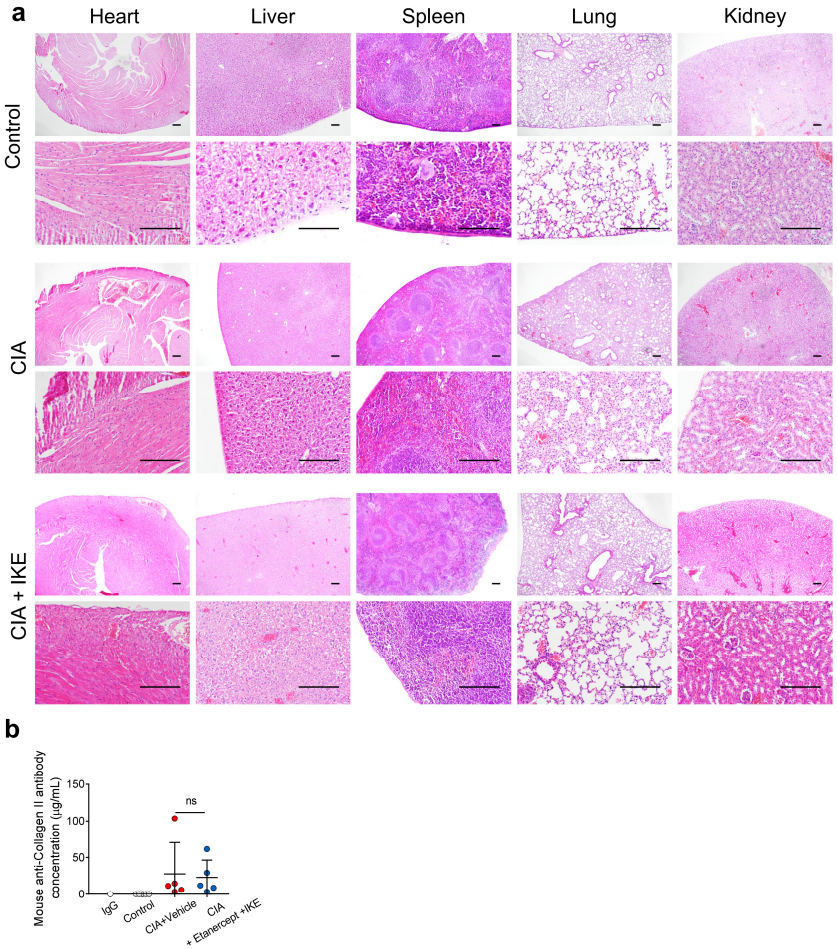

Supplementary Fig. 12. Pathological changes in organs of CIA mice treated with IKE. a H&E staining images of representative hearts, livers, spleens, lungs and kidneys in control and CIA mice treated with or without IKE (20 mg/kg, twice a week) for 36 days. Scale bars, 200 μm. Similar results were observed from all 5 mice tested for each group. **b** Detection of anti-type II collagen antibody in serum of CIA mice treated with etanercept in combination with IKE, performed with ELISA. n = 5 biologically independent animals per group. ns, P = 0.9612; two-tailed t test. Data are presented as mean ± SD. Source data are provided as a Source Data file.

Supplementary Table 1. Characteristics of rheumatoid arthritis (RA) individuals and osteoarthritis (OA) individuals for immunohistochemistry studies.

Characteristics	RA	OA
Number of patients	26	21
Age in years, median (IQR)	48.0 (39.5-54.3)	55.0 (49.5-57.0)
Female sex, (%)	14 (53.8)	12 (57.1)
Disease duration, year, median (IQR)	11 (6.8-15.0)	12 (7.0-15.0)
ESR, mm/hour, median (IQR)	52.5 (21.50-71.25)	19.0 (8.50-33.50)
DAS28, median (IQR)	5.76 (4.25-6.04)	na

Values are presented as median (interquartile range) or number (percentage). IQR, interquartile range, ESR, erythrocyte sedimentation rate; DAS28, 28-joint disease activity score; na, not applicable.

Supplementary Table 2. Characteristics of RA individuals for detection of MDA, 8-OHdG and iron levels in joint fluid.

Characteristics	RA
Number of patients	20
Age in years, median (IQR)	53.0 (50.0-61.3)
Female sex, (%)	16 (80.0)
Disease duration, year, median (IQR)	4.5 (1.1-9.8)
High diseases activity, (%)	12 (60)
Moderate diseases activity, (%)	8 (40)
ESR, mm/hour, median (IQR)	43.5 (31.25-56.25)
DAS28, median (IQR)	6.22 (4.85-6.43)

Values are presented as median (interquartile range) or number (percentage). IQR, interquartile range; ESR, erythrocyte sedimentation rate; DAS28, 28-joint disease activity score.

Supplementary Table 3. Characteristics of RA individuals for single-cell RNA sequencing.

Characteristics	RA
Number of patients	5
Age in years, average	49.8
Female sex, (%)	5 (100)
Disease duration, year, average	7.8
ESR, mm/hour, average	38.2
DAS28, average	6.61

Values are presented as average or number (percentage). ESR, erythrocyte sedimentation rate; DAS28, 28-joint disease activity score.

Supplementary Table 4. Characteristics of RA individuals for isolation of synovial fibroblasts from joint fluid and circulating fibrocytes from PBMC.

Characteristics	RA
Number of patients	6
Age in years, average	48.3
Female sex, (%)	4 (66.7)
Disease duration, year, average	0.7
ESR, mm/hour, average	47.17
DAS28, average	5.54

Values are presented as average or number (percentage). ESR, erythrocyte sedimentation rate; DAS28, 28-joint disease activity score.

Supplementary Table 5. The sequences of siRNA.

Names of siRNA primers	Sequences of primers
SLC40A1#1-sense	GGUGAGUGUUGUUAUAUAAUU
SLC40A1#1-antisense	UUAUAUAACAACA-CUCACCUU
SLC40A1#2-sense	GAGAGACUCYAGAAGUUAAUU
SLC40A1#2-antisense	UUAACUUCUAGAGUCUCUCCU
GCLC#1-sense	GCUAAUGAGUCUGACCAUUdTdT
GCLC#1-antisense	AAUGGUCAGACUCAUUAGC
GCLC#2-sense	GUAGUAUUCUGAACUACCUdTdT
GCLC#2-antisense	AGGUAGUUCAGAAUAUAUCdTdT
p65 #1-sense	GGACAUAUGAGACCUUCAAdTdT
p65 #1-antisense	UUGAAGGUCUCAUAUGUCCdTdT
p65 #2- sense	GAUGAGAUCUUCCUACUGUdTdT
p65 #2- antisense	ACAGUAGGAAGAUCUCAUdTdT
c-Jun #1- sense	CAGUGUUGUUUGGUAAAUAAGA
c-Jun #1- antisense	UUAUUUACAAACAACACUGGG
c-Jun #2- sense	GCUGAUUACUGUCAAUAAACA
c-Jun #2- antisense	UUUAUUGACAGUAAUCAGCUU
Negative Control sense	UUC UCC GAA CGU GUC ACG UTT
Negative Control antisense	ACG UGA CAC GUU CGG AGA ATT

Supplementary Table 6. The sequences of PCR primers.

Names of PCR primers	Sequences of PCR primers
huSLC40A1-Forward Primer	TGGATGGGTTCTCACTTCCTG
huSLC40A1-Reverse Primer	GTCAATCCTTCGTATTGTGGCAT
huMMP8 -Forward Primer	AAGTGGGAACGCACTAACTTG
huMMP8-Reverse Primer	GGATTCCATTGGGTCCATCAAAT
huMMP9-Forward Primer	TTCCCCTTCACTTTCCTGGGTA
huMMP9-Reverse Primer	CGCCACGAGGAACAAACTGTAT
huMMP11-Forward Primer	CCGCAACCGACAGAAGAGG
huMMP11-Reverse Primer	ATCGCTCCATACCTTTAGGGC
huMMP13-Forward Primer	TCTTCGGCTTAGAGGTGACTG
huMMP13-Reverse Primer	CAGAGGAGTTACATCGGACCA
huMMP14-Forward Primer	CATCTGTGACGGGAACTTTGA
huMMP14-Reverse Primer	GGCAGTGTTGATGGACGCA
GAPDH-Forward Primer	GCACCGTCAAGGCTGAGAAC
GAPDH-Reverse Primer	TGGTGAAGACGCCAGTGGA

Supplementary Table 7. Resource information for antibodies.

Antibody	Company	Cat#	Application	Dilution
FAP	Invitrogen	BMS168	TSA-based immunofluorescent multiplex	1:100
FAPα	Abcam	ab218164	TSA-based immunofluorescent multiplex	1:100
Mfap4	Thermo	PA5-24865	TSA-based immunofluorescent multiplex	1:100
Sparcl1	Santa Cruz	sc-514275	TSA-based immunofluorescent multiplex	1:100
F4/80	Cell Signaling Technology	#70076	TSA-based immunofluorescent multiplex	1:500
PerCP anti-CD3	Biolegend	317338	Flow cytometric analysis	5μl/test
PE anti-CD45	Biolegend	304008	Flow cytometric analysis	5μl/test
APC/Cyanine7 CD31	Biolegend	303120	Flow cytometric analysis	5μl/test
APC anti-CD68	Biolegend	333810	Flow cytometric analysis	5μl/test
PE/Cyanine7 anti-CD19	Biolegend	302216	Flow cytometric analysis	5μl/test
PE Goat anti-mouse IgG	Biolegend	405307	Flow cytometric analysis	5μl/test
PE anti-human CD14	Biolegend	367104	Flow cytometric analysis	5μl/test
FAP	Invitrogen	BMS168	Flow cytometric analysis	1:100
FITC anti-human CD90 (Thy1)	Biolegend	328107	Flow cytometric analysis	5μl/test
FITC anti-Collagen I	Sigma-Aldrich	FCMAB412F	Flow cytometric analysis	5μl/test
Dynabeads anti-CD19	Invitrogen	11143D	Isolation of circulating fibrocytes	Depletion: 50μl beads/2.5 x 10^7 cells/ml
Dynabeads anti-CD2	Invitrogen	11159D	Isolation of circulating fibrocytes	Depletion: 50μl beads/2.5 x 10^7 cells/ml
Dynabeads anti-CD14	Invitrogen	11149D	Isolation of circulating fibrocytes	Depletion: 50μl beads/2.5 x 10^7 cells/ml
SLC40A1	Abcam	ab78066	Western blotting	1:200
GCLM	HuaBio	ET1705-87	Western blotting	1:500

GCLC	HuaBio	ET1704-38	Western blotting	1:500
IκBα	HuaBio	ET1603-6	Western blotting	1:500
phospho-IκBα	HuaBio	ET1609-78	Western blotting	1:500
NF-kB p65	HuaBio	ET1603-12	Western blotting	1:500
SLC7A11	Abcam	ab175186	Western blotting	1:1000
c-Jun	Proteintech	24909-1-AP	Western blotting	1:1000
ferritin	Abcam	ab75973	Western blotting	1:1000
GAPDH	HuaBio	R1210-1	Western blotting	1:2000
β-actin	HuaBio	R1102-1	Western blotting	1:2000
4-HNE	Abcam	ab48506	Immunohistochemistry assay	1:25
4-HNE	Abcam	ab46545	Immunohistochemistry assay	1:50
PTGS2	Abcam	ab179800	Immunohistochemistry assay	1:500
GPX4	Abcam	ab125066	Immunohistochemistry assay	1:50
FAPα	Abcam	ab53066	Immunohistochemistry assay	1:50
GCLC	Abcam	ab53179	Immunohistochemistry assay	1:100
GCLM	Abcam	ab126704	Immunohistochemistry assay	1:50
p-NF-κB p65	Thermo Fisher	44-711G	Immunohistochemistry assay	1:50
8-OHdG	Abcam	ab48508	Immunohistochemistry assay	1:100
VCAM-1	Abcam	ab134047	TSA-based immunofluorescent multiplex	1:500
4-HNE	Abcam	ab46545	TSA-based immunofluorescent multiplex	1:50
CD248	Abcam	ab217535	TSA-based immunofluorescent multiplex	1:200
TNFR1	Sino Biological	10872-R111	blocking	1:400
TNFR2	Sino Biological	10417-R00N6	blocking	1:200
rabbit IgG Isotype Control	Invitrogen	31235	IgG Isotype Control	1:100
mouse IgG Isotype Control	Invitrogen	14-4714-82	IgG Isotype Control	1:100